# Time Evolution of Quantum Entanglement of an EPR Pair in a Localized Environment

Jia Wang, Xia-Ji Liu, and Hui Hu
*Centre for Quantum and Optical Science, Swinburne University of Technology, Melbourne 3122, Australia*
(Dated: January 25, 2017)

The Einstein–Podolsky–Rosen (EPR) pair of qubits plays a critical role in many quantum protocol applications such as quantum communication and quantum teleportation. Due to interaction with the environment, an EPR pair might lose its entanglement and can no longer serve as useful quantum resources. On the other hand, it has been suggested that introducing disorder into environment might help to prevent thermalization and improve the preservation of entanglement. Here, we theoretically investigate the time evolution of quantum entanglement of an EPR pair in a random-field XXZ spin chain model in the Anderson localized (AL) and many-body localized (MBL) phase. We find that the entanglement between the qubits decreases and approaches to a plateau in the AL phase, but shows a power-law decrease after some critical time determined by the interaction strength in the MBL phase. Our findings, on one hand, shed lights on applying AL/MBL to improve quantum information storage; on the other hand, can be used as a practical indicator to distinguish the AL and MBL phase.

arXiv:1701.03565v2 [quant-ph] 24 Jan 2017

An Einstein-Podolsky-Rosen (EPR) pair is a pair of qubits which are in maximally entangled state. Due to their perfect quantum correlations, EPR pairs lie at the heart of many important proposals for quantum communication and computation, such as quantum teleportation [1, 2]. In reality, however, due to the unavoidable decoherence induced by the couplings to the surrounding environment, an EPR pair might become a state $\rho$ that lose entanglement after a certain time, making this qubit pair no longer useful as a quantum resource. One of the main tool to overcome the decoherence is a protocol named entanglement distillation [3, 4]. This method can be used to transform $N$ copies of less entangled states $\rho$ back into a smaller number $m$ of approximately pure EPR pairs by using only local operations and classical communication (LOCC), where the ratio $m/N$ depends on the amount of entanglement left in $\rho$. Therefore, it is of great interest to design quantum information storage devices that can keep a strong quantum entanglement for a long time to improve the distillation efficiency. In this Letter, we study the possibility of preserving quantum entanglement in a localized environment by introducing strong disorder.

The idea that disorder can help protecting initial correlations and information is first raised by Anderson in 1958. He focused on the behaviors of non-interacting particles experiencing random potentials, which is now named as Anderson localization (AL) [5]. In AL, the diffusion of particle's wave-packet in a disordered environment is absent, implying the initial information of particle's position is "remembered". Extending this concept to an interacting system, namely many-body localization (MBL), has attracted many people's interest including Anderson himself. Recently, this field attracts an intense attraction [6–8], partially due to the lately rapid progress in ultracold atomic experiments that has made quantum isolated many-body systems with tunable interaction and disorder available, including ultracold atoms in optical lattices [9–11] and ion traps [12]. These experimentally available systems constitute promising platforms for exploring the AL and MBL localization phases and stimulated a series of theoretical studies. Many remarkable properties of these localized phases have ever since been theoretically predicted: Poisson distributions of energy gap [13, 14], absences of transportation of charge, spin, mass or energy even at high temperature [15–17], protecting quantum order and discrete symmetry that normally only exists in the ground state [18–21] and existence of mobility edge [22–24]. In particular, quantum entanglement has been discovered to play very important roles in identifying different phases: energy eigenstates in localized phases have area-law bipartition entanglement entropy in contrast to the volume-law entropy of a thermalized state [25, 26]. In addition, after a sudden (global or local) quench, the entanglement shows a fast power-law spreading in a thermal phase, but only a slow logarithmic spreading in an MBL phase and no spreading at all in an AL phase [27–29]. The slow entanglement spreading in the localized phases is restricted by a variant of the Lieb-Robinson bound on the information light cone, which can in principle be observed via out-of-time-order correlations (OTOC) [30–32]. This slow spreading of entanglement also suggests that the local correlations might be maintained for a long time in a localized environment, which has a potential application in quantum information storage. Indeed, it has been shown that deep in the localized phase, the quantum coherence of local degrees of freedom, e.g. a single qubit, has been demonstrated to be maintained for a very long time [33–35]. However, to the best of our knowledge, whether disorder can also help to protect quantum entanglement between qubits has never been directly studied. In this Letter, we focus on studying the time evolution of the quantum entanglement between an EPR pair shared by two observers namely Alice and Bob and coupled to a localized environment.

As a concrete example, we conduct our analysis in a prototype Hamiltonian that has been studied extensively in the MBL literature: a one-dimensional (1D) $s = 1/2$ spin chain XXZ Hamiltonian with nearest neighbor interactions

$$H = \sum_i J\left(s_i^x s_{i+1}^x + s_i^y s_{i+1}^y\right) + \Delta s_i^z s_{i+1}^z + h_i s_i^z, \quad (1)$$

where $J$ and $\Delta$ are both constant, and $h_i$ are random fields uniformly distributed over $[-h, h]$. The total magnetization $S_z \equiv \sum_i s_i^z$ is a good quantum number, and hence we will restrict our calculation for $S_z = 0$ hereafter. We want to emphasize here that the spin-spin interacting Hamiltonian is chosen not only because its localized phase has been well studied, but also because in some reality cases, the main source of decoherence for qubits are from their interaction with unwanted environment spins. We also remark here that, the Hamiltonian in Eq. (1) can be mapped into a Fermi-Hubbard model using a Jordan-Wigner transformation, where $J$ is equivalent to the hopping coefficient and $\Delta$ is equivalent to the interaction strength. Thus with strong enough disorder $h$, the spin chain is expected to be in the AL (MBL) phase for $\Delta = 0$ ($\Delta \neq 0$) respectively.

Here, we prepare an initial state in the form of $|\Psi(0)\rangle = |\mathrm{EPR}\rangle_{\mathrm{AB}} \otimes |\mathrm{NEEL}\rangle_E$, where the subscript A stands for Alice's spin, B stands for Bob's, and E stands for all the other spins serving as an environment. The environment is prepared in a Néel's state mimicking a high-temperature environment and is initially *not* entangled with the EPR pair of the spin A and B. We then study the time evolution of this state under the Hamiltonian in Eq. (1) using exact diagonalization, obtaining the reduced density matrix $\rho$ of the spin pair A and B by tracing out all the environment spins and calculating quantum entanglement measurements that are usually averaged over many realizations of disorder (typically 1000 times). The quantum entanglement measurement we focus here is the logarithmic negativity is given by $S_N = \log_2(N + 1)$, where $N$, namely negativity, is a measure related to the Peres-Horodecki criterion: $N = 2\sum_i \max(0, -\mu_i)$ [36, 37]. Here $\mu_i$'s are the eigenvalues of $\rho^\Lambda$ who is the partial transpose of $\rho$. We would like to remark here that, the logarithmic negativity, even though lacks convexity, is a full entanglement monotone that does not increase on average under a general positive partial transpose (PPT) preserving operation as well as local operations and classical communication (LOCC) [38]. In addition, the logarithmic negativity serves as the upper bound of distillable entanglement that limits the amount of nearly maximally entangled qubit pairs that can be asymptotically distilled from $N$ copies of $\rho$ via quantum distillation [3, 4].

In our current set-up, two scenarios can be studied: in the first scenario shown in Fig. 1(a), Bob is isolated from the environment, which resembles a quantum communication or quantum teleportation situation; in the second scenario illustrated in Fig. 1(b), both Alice and Bob are in contact with the same environment mimicking a quantum calculation realization. Our numerical result shows that the entanglement evolutions in both scenarios have similar qualitative behavior. Therefore, we focus on discussing the logarithmic negativity for scenario one here. These discussion and conclusions are however applicable for other entanglement measurements such as concurrence and entanglement of formation in both scenarios [39].

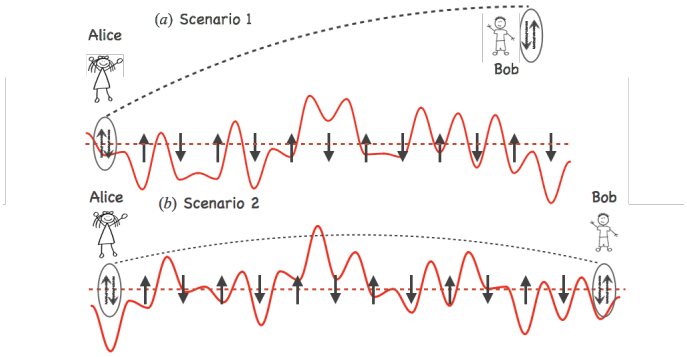


Figure 1. A sketch of the two scenarios that studied here. (a) The first scenario, where both Alice and Bob's spins are immersed in the same disordered environment. (b) The second scenario, where Bob is isolated from the environment that Alice experiences.

Figure 2 shows our main result, the logarithmic negativity between Alice and Bob as a function of time in the scenario one, with the disorder strength $h = 3J$ for different numbers of spins $L$ (including Alice and Bob's spins) and $\Delta = 0$ ($10^{-2}$) for the AL (MBL) phases. Initially, the entanglement is prepared at maximum $S_N(0) = 1$. At around $t \approx 1/J$, the entanglement in both AL and MBL phases shows a power-law decay following some oscillations, which has been recognized as the diffusion of initial state to a size of the localization length. After about a critical time $t_c \approx 1/\Delta$, the entanglement of MBL and AL shows dramatically different behavior. The entanglement in AL phases converges to a plateau independent of the spin chain size $L$, where all curves for different $L$ are visually overlapping. In contrast, the entanglement in MBL phases shows a power law decay $\sim t^{-v}$ with $v > 0$, which is emphasized by the linear behavior on a log-log scale in Fig. 2.

Due to the finite size of our system, the entanglement in MBL phases will eventually also saturate to some constants after a very long time. Nevertheless, as illustrated in the inset of Fig. 2, the final saturated values are shown to decrease exponentially as a function of spin chain size $\sim \exp(-\beta L)$, where $\beta$ is a constant. From these observations, one can expect that the entanglement in AL phase

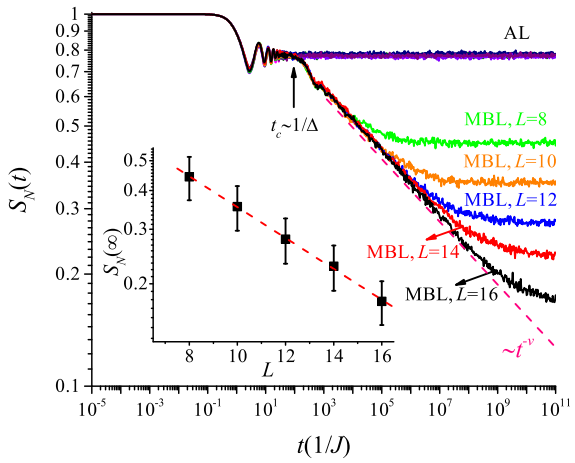


Figure 2. Logarithmic negativity in AL ($\Delta = 0J$) and MBL ($\Delta = 10^{-2}J$) phases as a function of time for disorder strength $h = 3$ and different spin chain length $L$. The dashed line helps to highlight the power-law decay behavior in the MBL phases. The inset shows the final saturation values of entanglement $S_N(\infty)$ in MBL phases as a function of $L$, where the error bar shows the variance from averaging over different disorder realizations. The dashed line shows a exponential fit of $S_N(\infty) \sim \exp(-L)$.

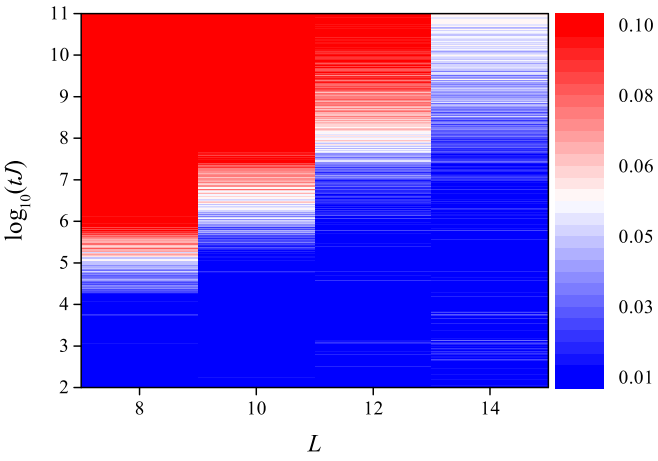


Figure 3. Color plot of $\Delta S_N^{(L)}$ defined in the main text. The red color indicates a large value of $\Delta S_N^{(L)}$, which is constrained by a logarithmic light cone.

will never reduce to zero, but a constant depend only on disorder strength even in the thermodynamic limit $L \to \infty$. On the other hand, no matter how small the interaction strength $\Delta$ is, the entanglement will be completely dissipated after infinite long time in the thermodynamic limit. However, this dissipation is very slow if the disorder is strong enough. In addition, the entanglement of AL phase and MBL phase only become different abruptly after the critical time $t_c$, therefore, if $\Delta$ is small, the entanglement can still be preserved in the AL level before $t_c$.

Therefore, we can conclude that the AL phase is ideal for creating quantum storage devices to preserve quantum entanglement between a qubit pair. On the other hand, if a weak interaction strength $\Delta$ is unavoidable in the system, the MBL phase can still be applied to preserve entanglement but with an expiration time $t_c$. However, one must carry an entanglement distillation to use the qubit pair before conducting quantum protocols. We also wish to emphasize here that the preservation of entanglement between two qubits in a localized environment is, of course, not better than in a completely decoupled environment. However, in a realistic situation where coupling between the qubit pair and the environment cannot be eliminated, our study provides a generic way of preserving entanglement without a specific fine tuning of the Hamiltonian but simply introducing strong enough disorder into the environment.

Our results can also be directly applied to identify the localized phase being AL or MBL. Most of previous such studies have been focused on studying the bipartite entanglement (, i.e. dividing the system into two subsystems,) of an initial product state after global quench or an energy eigenstate after a local quench [27–29]. Nevertheless, the experimental observation of bipartite entanglement in principle can be very challenging for a large system and may even be impossible in the thermodynamic limit. On the other hand, measuring entanglement between local degrees of freedom in an optical lattice [40] and trap ions [41, 42] has been reported lately. Therefore, studies of entanglement between two sites have been investigated recently, motivated by the fact that such entanglement between local degrees of freedom is much more experimentally accessible [43–45]. These studies usually focus on the case where the initial state is a product state, and a temporary entanglement generated due to initial diffusion. The AL and MBL features are analyzed by the following decay of this temporary entanglement that decreases exponentially as a function of distances between sites in the deep localized phase. Therefore, these studies are usually limited to entanglement between nearest few sites. Our methods, using an initial prepared EPR pair, can in principle overcomes these limitations and be experimentally accessible.

Our study also gives an interesting insight into the nature of entanglement spread in MBL phases. The power law decay and the saturated values of entanglement in MBL phases suggest that we can define a saturation time scale $t_s$, where the entanglement in MBL phases is about to be saturated, as $v \log(t_s) \sim L$, which resembles the logarithmic light-cone found in previous bipartite entanglement studies [27–29]. This logarithmic light-cone can be understood from the modified Lieb-

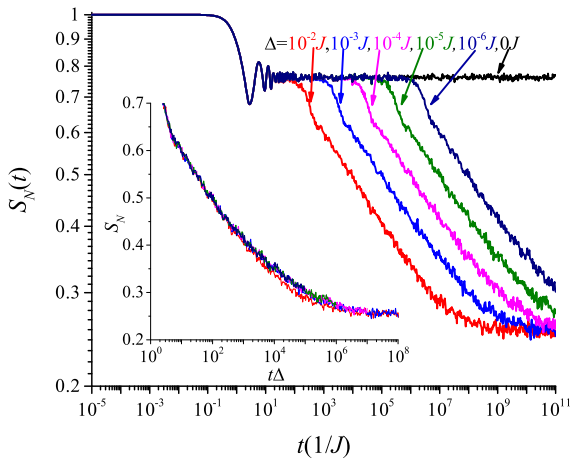


Figure 4. Entanglement decay for different interaction strength $\Delta$. Here, the size of spin chain $L = 12$ and $h = 3J$. The inset shows the long-time behavior of entanglement as a universal function of $t\Delta$.

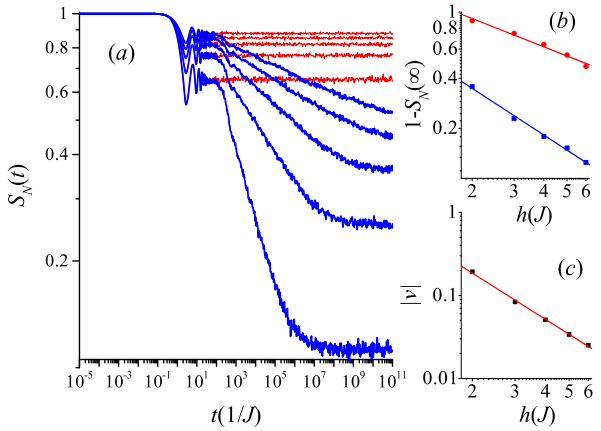


Figure 5. (a) Entanglement decay for different disorder strength $h$ with $L = 12$ and $\Delta = 10^{-2}J$. The red thin (blue thick) curves represents AL (MBL) phases for $h = 2J, 3J, 4J, 5J, 6J$ from bottom to top. (b) The saturated value $1 - S_N(\infty)$ as a function of $h$, the red circles (blue squares) represent AL (MBL) phase, wher the solid lines are power-law fit $1 - S_N(\infty) \sim h^c$ . (c) The symbols are the decay index $v$ as a function of $h$, and the solid line is a power-law fit.

Robinson bound of information spreading (in this case entanglement spreading) [46]. One convenient and common way to describe the Lieb-Robinson bound is to compare the time-evolution of a local observable $A$ under the full Hamiltonian with its time-evolution under a truncated Hamiltonian that only includes interactions contained in a region of distance no more than $L$. Even though entanglement is technically not an observable, we study the quantity $\Delta S_N^{(L)} = S_N^{(L=16)} - S_N^{(L)}$ under the same spirit. In scenario two, this quantity can be interpreted as the differences of entanglement between a full spin chain of $L = 16$ and a truncated spin chain $L$ near Alice's spin. The result is shown in Fig. 3, where one can directly see that the significant differences are constrained within a logarithmic light cone. This is a direct evidence that entanglement is spreading logarithmically in an MBL phase suggested by previous OTOC studies [30–32].

We further take a qualitative analysis of the effects of interaction strength $\Delta$ and disorder strength $h$ on the decay of entanglement. Figure 4 shows the entanglement decay for different $\Delta$, confirming that entanglement in AL and MBL phases only become different abruptly after the critical time $t_c \approx 1/\Delta$. Furthermore, the saturated value in the MBL phases does not variate appreciably for different $\Delta$. In fact, the logarithmic entanglement for $t \gg t_c$ is a universal function of $t\Delta$ as evidenced by the inset of Fig. 4. Finally, Fig. 5(a) shows the entanglement decay for different $h$, where the decay rate becomes slower and the saturated value becomes larger for a stronger disorder. As a result of the competition of these two effects, the saturation time becomes longer, suggesting that a stronger disorder is beneficial for storing EPR pairs. Our numerical results also show that the decrease of entanglement at infinite long time $1 - S_N(\infty)$ and the decay index $v$ are both has a power-law dependence on $h$, as shown in Fig. 5 (b) and (c). This analysis can be interpreted as a stronger disorder and weaker interaction is beneficial for preserving quantum entanglement, which is consistent with our expectation.

In summary, we studied the time evolution of quantum entanglement of an EPR pair coupling to a localization environment. This study allows us to explored the possibility and limitation of applying localization phase to preserve quantum entanglement between qubit pairs. Our results can also be regarded as an experimentally accessible protocol to discriminate AL and MBL phases, and understand the nature of entanglement propagation in these systems.

This research was supported under Australian Research Council's Future Fellowships funding scheme (project number FT140100003) and Discovery Projects funding scheme (project number DP170104008). The numerical calculations were partly performed using Swinburne new high-performance computing resources (Green II).

[1] A. K. Ekert, Phys. Rev. Lett. **67**, 661 (1991).
[2] C. H. Bennett, G. Brassard, C. Crépeau, R. Jozsa, A. Peres, and W. K. Wootters, Phys. Rev. Lett. **70**, 1895 (1993).
[3] C. H. Bennett, G. Brassard, S. Popescu, B. Schumacher,

J. A. Smolin, and W. K. Wootters, Phys. Rev. Lett. **76**, 722 (1996).
[4] M. Horodecki, P. Horodecki, and R. Horodecki, Phys. Rev. Lett. **80**, 5239 (1998).
[5] P. W. Anderson, Phys. Rev. **109**, 1492 (1958).
[6] D. M. Basko, I. L. Aleiner, and B. L. Altshuler, Ann. Phys. (N.Y.) **321**, 1126 (2006).
[7] E. Altman and R. Vosk, Annu. Rev. Condens. Matter Phys. **6**, 383 (2015).
[8] R. Nandkishore and D. A. Huse, Annu. Rev. Condens. Matter Phys. **6**, 15 (2015).
[9] M. Schreiber, S. S. Hodgman, P. Bordia, H. P. Lueschen, M. H. Fischer, R. Vosk, E. Altman, U. Schneider, and I. Bloch, Science **349**, 842 (2015).
[10] P. Bordia, H. P. Luschen, S. S. Hodgman, M. Schreiber, I. Bloch, and U. Schneider, Phys. Rev. Lett. **116**, 140401 (2016).
[11] J.-y. Choi, S. Hild, J. Zeiher, P. Schauss, A. Rubio-Abadal, T. Yefsah, V. Khemani, D. A. Huse, I. Bloch, and C. Gross, Science **352**, 1547 (2016).
[12] J. Smith, A. Lee, P. Richerme, B. Neyenhuis, P. W. Hess, P. Hauke, M. Heyl, D. A. Huse, and C. Monroe, Nat. Phys. **12**, 907 (2016).
[13] V. Oganesyan and D. A. Huse, Phys. Rev. B **75**, 155111 (2007).
[14] Y. Y. Atas, E. Bogomolny, O. Giraud, and G. Roux, Phys. Rev. Lett. **110**, 084101 (2013).
[15] T. C. Berkelbach and D. R. Reichman, Phys. Rev. B **81**, 224429 (2010).
[16] D. Pekker, G. Refael, E. Altman, E. Demler, and V. Oganesyan, Phys. Rev. X **4**, 011052 (2014).
[17] K. Agarwal, S. Gopalakrishnan, M. Knap, M. Müller, and E. Demler, Phys. Rev. Lett. **114**, 160401 (2015).
[18] D. A. Huse, R. Nandkishore, V. Oganesyan, A. Pal, and S. L. Sondhi, Phys. Rev. B **88**, 014206 (2013).
[19] Y. Bahri, R. Vosk, E. Altman, and A. Vishwanath, Nat. Commun. **6**, 7341 (2015).
[20] B. Bauer and C. Nayak, J. Stat. Mech. , P09005 (2013).
[21] A. Chandran, V. Khemani, C. R. Laumann, and S. L. Sondhi, Phys. Rev. B **89**, 144201 (2014).
[22] D. J. Luitz, N. Laflorencie, and F. Alet, Phys. Rev. B **91**, 081103 (2015).
[23] X. Li, S. Ganeshan, J. H. Pixley, and S. Das Sarma, Phys. Rev. Lett. **115**, 186601 (2015).
[24] E. Baygan, S. P. Lim, and D. N. Sheng, Phys. Rev. B **92**, 195153 (2015).
[25] M. Žnidarič, T. Prosen, and P. Prelovšek, Phys. Rev. B **77**, 064426 (2008).
[26] J. A. Kjäll, J. H. Bardarson, and F. Pollmann, Phys. Rev. Lett. **113**, 107204 (2014).
[27] J. H. Bardarson, F. Pollmann, and J. E. Moore, Phys. Rev. Lett. **109**, 017202 (2012).
[28] M. Serbyn, Z. Papić, and D. A. Abanin, Phys. Rev. Lett. **110**, 260601 (2013).
[29] D.-L. Deng, X. Li, J. H. Pixley, Y.-L. Wu, and S. D. Sarma, "Logarithmic entanglement lightcone in many-body localized systems," (2016), arXiv:1607.08611.
[30] Y. Huang, Y.-L. Zhang, and X. Chen, "Out-of-time-ordered correlator in many-body localized systems," (2016), arXiv:1608.01091.
[31] R. Fan, P. Zhang, H. Shen, and H. Zhai, "Out-of-time-order correlation for many-body localization," (2016), arXiv:1608.01914.
[32] X. Chen, T. Zhou, D. A. Huse, and E. Fradkin, "Out-of-time-order correlations in many-body localized and thermal phases," (2016), arXiv:1610.00220.
[33] M. Serbyn, M. Knap, S. Gopalakrishnan, Z. Papić, N. Y. Yao, C. R. Laumann, D. A. Abanin, M. D. Lukin, and E. A. Demler, Phys. Rev. Lett. **113**, 147204 (2014).
[34] Y. Bahri, R. Vosk, E. Altman, and A. Vishwanath, Nat. Comm. **6**, 7341 (2015).
[35] R. Vasseur, S. A. Parameswaran, and J. E. Moore, Phys. Rev. B **91**, 140202 (2015).
[36] A. Peres, Phys. Rev. Lett. **77**, 1413 (1996).
[37] M. Horodecki, P. Horodecki, and R. Horodecki, Phys. Lett. A **223**, 1 (1996).
[38] M. B. Plenio, Phys. Rev. Lett. **95**, 090503 (2005).
[39] See Supplemental Material at [PRL will be inserted by publisher] for entanglement measurements such as concurrence and entanglement of formation in scenario two.
[40] T. Fukuhara, S. Hild, J. Zeiher, P. Schauß, I. Bloch, M. Endres, and C. Gross, Phys. Rev. Lett. **115**, 035302 (2015).
[41] P. Jurcevic, B. P. Lanyon, P. Hauke, C. Hempel, P. Zoller, R. Blatt, and C. F. Roos, Nature (London) **511**, 202 (2016).
[42] E. A. Martinez, C. A. Muschik, P. Schindler, D. Nigg, A. Erhard, M. Heyl, P. Hauke, M. Dalmonte, T. Monz, P. Zoller, and R. Blatt, Nature (London) **534**, 516 (2016).
[43] S. Bera and A. Lakshminarayan, Phys. Rev. B **93**, 134204 (2016).
[44] G. D. Tomasi, S. Bera, J. H. Bardarson, and F. Pollmann, "Quantum mutual information as a probe for many-body localization," (2016), arXiv:1608.07183.
[45] F. Iemini, A. Russomanno, D. Rossini, A. Scardicchio, and R. Fazio, "Signatures of many-body localisation in the dynamics of two-sites entanglement," (2016), arXiv:1608.08901.
[46] M. Friesdorf, A. H. Werner, W. Brown, V. B. Scholz, and J. Eisert, Phys. Rev. Lett. **114**, 170505 (2015).

## SUPPLEMENTAL MATERIAL

It is well known that von Neumann entropy is not a valid entanglement measurement if the collective states are in mix states. However, several entanglement measurement have been found for a pair of qubits, including concurrence, negativity and their close relatives: entropy of formation and logarithmic negativity. These entanglement measurements are "good" in the following sense: (i) for a maximally entangled state, i.e. an EPR pair, these measurements reach their maximum values (equal one in our definitions); (ii) for collective seperable states, these measurements vanish; (iii) is a continuous function of density matrices of the two-qubit states. Notice that these measurements, however, does not nessesarily give same ordering for different entangled states.

Let us first give the defination of the entanglement measurements mentioned above. Denoting the collective state for two selected qubits by a density matrix $\rho$, the concurrence is given by $C = \max(\sqrt{\lambda_1} - \sqrt{\lambda_2} - \sqrt{\lambda_3} - \sqrt{\lambda_4})$, where $\lambda_i$'s are the eigenvalues of $\rho\tilde{\rho}$ in decending order and $\tilde{\rho} \equiv \sigma^y \otimes \sigma^y \rho^* \sigma^y \otimes \sigma^y$. Concurence is monotonically related to the entangelment of formation by the Wootters formula $S_F = h\left[\left(1+\sqrt{1-C^2}\right)/2\right]$, where $h(x) = -x\log_2 x - (1-x)\log_2(1-x)$. Negativity is a measure related to the Peres-Horodecki criterion: $N = 2\sum_i \max(0, -\mu_i)$, where $\mu_i$'s are the eigenvalues of $\rho^\Lambda$ who is the partial transpose of $\rho$. The logarithmic negativity is then given by $S_N = \log_2(N+1)$.

In the main text, we show that the time evolution of logarithmic negativity between a pair of qubits that initially prepared to be as an EPR pair in scenario one. Here, we present results of other entanglement measures in scenario two and show that these measurements are qualitatively similar, and serve the same role in our analysis. Therefore, the discussions and conclusions of logarithmic negativity in scenario one are also applicable for all measurements in scenario two.

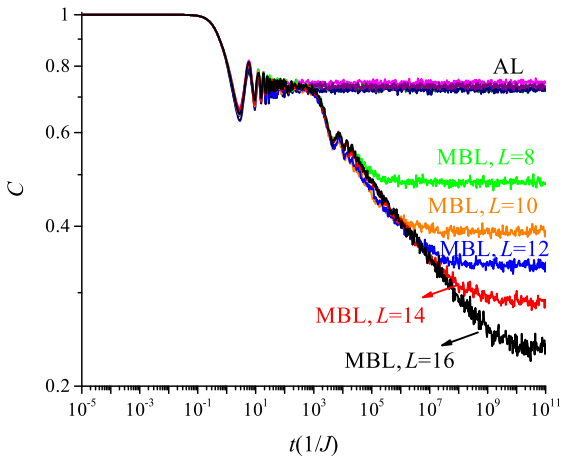


Figure 6. Concurrence as a function of time for disorder strength $h = 5$ and interaction strength $\Delta = 0J(10^{-3}J)$ for AL (MBL) phases. The results for AL phases with different spin chain length $L$ are almost overlapping each other, and the results for different MBL phases are indicated in the figure.

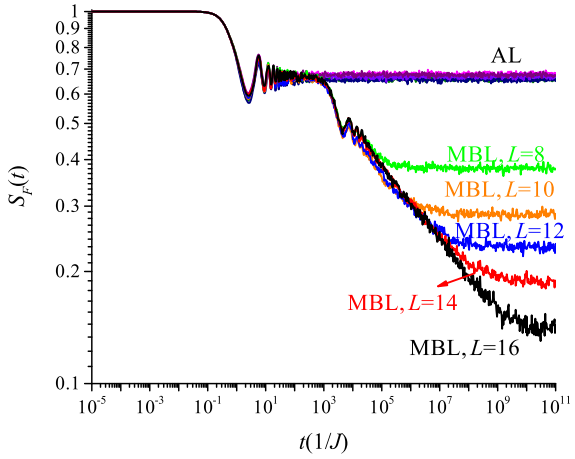


Figure 7. Entropy of formation as a function of time for disorder strength $h = 5$ and interaction strength $\Delta = 0J(10^{-3}J)$ for AL (MBL) phases. The results for AL phases with different spin chain length $L$ are almost overlapping each other, and the results for different MBL phases are indicated in the figure.

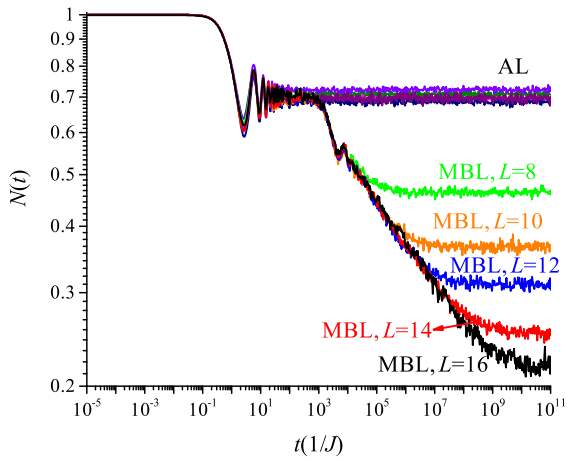


Figure 8. Negativity s a function of time for disorder strength $h = 5$ and interaction strength $\Delta = 0J(10^{-3}J)$ for AL (MBL) phases. The results for AL phases with different spin chain length $L$ are almost overlapping each other, and the results for different MBL phases are indicated in the figure.

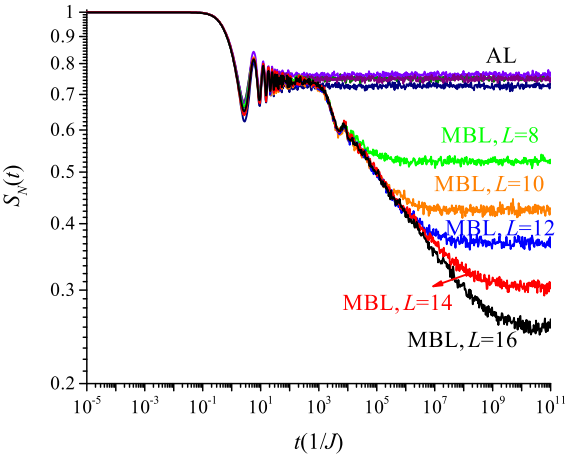


Figure 9. Logarithmic negativity s a function of time for disorder strength $h = 5$ and interaction strength $\Delta = 0J(10^{-3}J)$ for AL (MBL) phases. The results for AL phases with different spin chain length $L$ are almost overlapping each other, and the results for different MBL phases are indicated in the figure.